Analysis of Sawtooth Oscillations Using Simultaneous Measurement of Electron Cyclotron Emission Imaging and X-Ray Tomography on TFTR

Y. Nagayama,[a] K. M. McGuire, M. Bitter, A. Cavallo, E. D. Fredrickson, K. W. Hill, H. Hsuan, A. Janos, W. Park, G. Taylor, and M. Yamada

Princeton Plasma Physics Laboratory, P.O. Box 451, Princeton, New Jersey 08543

(Received 20 March 1991)

High-resolution electron cyclotron emission and x-ray image reconstructions have been made simultaneously during the sawtooth crash in the fast rotating plasma with neutral beam injection heating on TFTR. The measured x-ray emission is identified as metal impurity radiation. The results suggest that the sawtooth crash is a full reconnection process for the TFTR sawteeth. The crescent-shaped "hot spot" in the x-ray emissivity is found not to represent flux surfaces. New features are observed during the sawtooth crash, such as an oval-shaped hot spot and a cooler region between the island and the hot spot.

PACS numbers: 52.25.Fi, 42.30.Wb, 52.25.Nr, 52.55.Fa

Periodic crashes of the central electron temperature, called sawtooth oscillations, are a common feature of tokamak discharges. Kadomtsev explained the sawtooth crash with a resistive reconnection model [1]. The JET experiment showed disagreements between this model and fast sawtooth crash on big tokamaks [2]. In this paper, we report the simultaneous measurements of electron cyclotron emission (ECE) imaging and x-ray tomography during sawtooth crash, which describe a fast full reconnection process on TFTR. The significant findings are as follows: (1) The x rays are identified as metal impurity emission; (2) the crescent-shaped "hot spot" in the x-ray image does not show kink flow but describes that the impurity convection is slower than the electron heat conduction; (3) x-ray emission contours do not always represent flux surfaces; and (4) the shrinking circular hot spot and the growing crescent-shaped island appear in the electron temperature contours, which are considered to be the best representation of flux surfaces. New features of the sawtooth crash are also revealed from the high-resolution image reconstruction. For effective documentation, we sample sawtooth crashes whose crash time is short in terms of impurity transport but is longer than the plasma rotation period. The features for the full reconnection process are observed in other TFTR fast sawtooth crashes. This fast reconnection has been of strong interest in the plasma physics community [3].

We apply the ECE and x-ray image reconstruction techniques to a typical TFTR fast sawtooth crash in a plasma with major radius of 2.45 m, minor radius of 0.80 m, toroidal magnetic field of 4.8 T at $R=2.45$ m, plasma current of 1.6 MA, heated by cotangential (in the direction of plasma current) neutral beam injection (NBI) of 12.5 MW, and countertangential NBI of 4.5 MW. This plasma has a central ion temperature of 17 keV, central electron temperature of 6.8 keV, volume averaged density of $\langle n_e\rangle = 3.2\times10^{19}$ m^{-3}, density peakedness of $n_{e0}/\langle n_e\rangle = 1.9$, and fast ion beam density of 20% of the electron density at the center.

The electron temperature profile on the midplane of the plasma is measured with a twenty-channel grating polychromator [4]. The polychromator data are cross-calibrated to a Michelson interferometer [5]; although the uncertainty of absolute temperature is (5–10)%, the point-to-point relative error is less than 2%. The data are collected with a 2-μs time resolution covering $R=2.2$–3.4 m with a channel separation of 6 cm (each channel has a radial resolution of 3 cm). The poloidal resolution of the reconstructed image is 11°. The data from the inside and outside major radii are used for a full rotation (66 μs), and an interpolation between both sides is carried out, so that the time resolution is better than 33 μs [6]. In addition, two soft-x-ray cameras separated by 75° view the plasma, one vertically and the other horizontally, through 125-μm-thick Be filters with twenty and sixty silicon-diode detectors, respectively [7,8]. With this Be filter, the sensitivity of x ray between 3 and 15 keV is higher than 50% of its maximum [7]. As described in Ref. [9], the x-ray emission is characterized by a Fourier series of order of 7 and Bessel function expansions of order of 10. The data are taken in a quarter rotation using two cameras, so the time resolution is 17 μs. The effective radial resolution is 9 cm and the poloidal resolution 13°. The image reconstruction techniques using rotation have been reported previously together with an analysis of the reconstruction errors due to the noise and the rigid rotation assumptions using numerical simulations [6].

The ECE and x-ray signals for sawtooth oscillations are shown in Fig. 1. The ECE and x-ray images with the inversion surface superimposed are shown in Figs. 2 and 3, at the times indicated by the letters in Fig. 1. Here, the inversion surface is obtained from the electron temperature profile as in the previous report [10]. The time evolution of the ECE image, which is considered to represent the evolution of flux surfaces, is shown in Fig. 2. The sawtooth crash starts at time D and finishes at time K in Fig. 1, so that the crash time is about 400 μs, which is longer than the central temperature decay time of 200 μs (from D to G in Fig. 1). The crash time is 10 times faster than the Kadomtsev time [1]. Figure 2 clearly

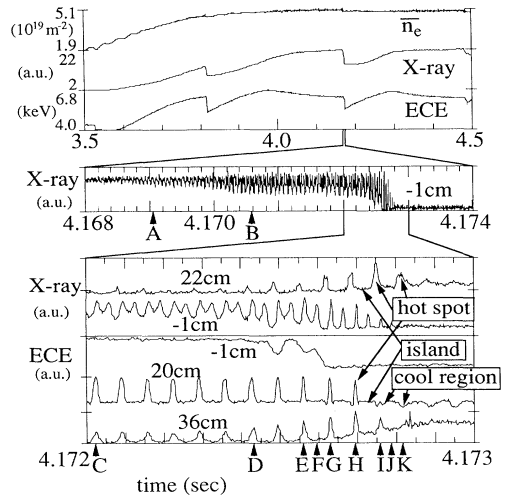

FIG. 1. The ECE signal from the grating polychromator and the x-ray signals from the horizontal camera during a sawtooth oscillation. Here, minor radii are measured from the magnetic axis, and the negative sign indicates the high-field side on the ECE signals. The parameter of the x-ray channel indicates the height of the x-ray chord. The sharp positive spike corresponds to the "hot spot," the flat region between the spikes to the "island," and the negative dip to the "cool region." The pulse width corresponds to the width in the poloidal direction in the 2D tomographic image.

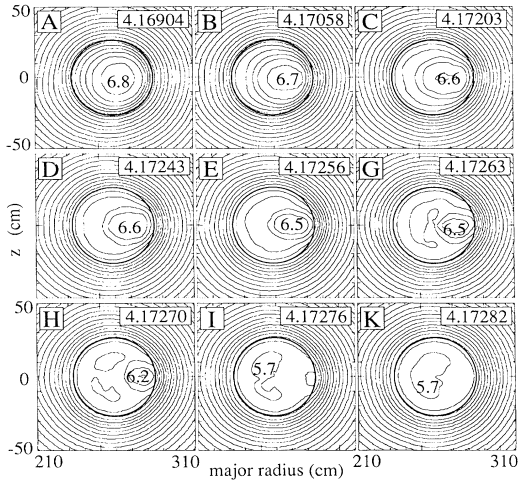

FIG. 2. Series of ECE images during the sawtooth crash. The number on the center indicates peak electron temperature in keV. The contour step size is 300 eV. The bold circular line indicates the inversion radius which is obtained from the ECE signals. The numbers on the right of the figures indicate the reconstruction time in seconds.

shows a growing crescent-shaped island and a shrinking hot spot, as expected from a full reconnection process [1]. The same process is also observed for a faster sawtooth crash having the central temperature decay time of 37 μs. The crash time is 180 μs, which is 20 times faster than the Kadomtsev time. A correlation between the crash time and the resistivity is not found for sawteeth on TFTR.

We now compare images from ECE and x-ray reconstructions (Fig. 3). In Fig. 3, the "ECE (perturbation)" is the residual of the averaged signal over one cycle of the rotation subtracted from the raw signal, and it is more sensitive to the presence of perturbations. We also compare the images when the hot spot is on the weak-field side (larger-major-radius side) (Fig. 2, frames E and G) and on the strong-field side (smaller-major-radius side) (Fig. 3, frame F). Here, we note that the fine structure in the x-ray image is an artifact introduced by the limited number of Fourier components.

Three important features can be identified in the high-resolution image reconstructions: (1) The hot spot pushes out more on the weak-field side; (2) a "cool region" between the hot spot and the island grows gradually; and (3) the shape of the hot spot is oval and radially elongated before the crash phase. Theoretically, the pushing out of the hot spot on the weak-field side can be explained as a combination of finite pressure and toroidal effects [10,11]. The cool region, which also can be seen in the raw data traces (Fig. 1), is not due to the heating of the island, because the temperature of the island does not change (Fig. 1). The cool region becomes an $m=1$, $n=1$ "cold bubble" after the crash, which sometimes generates successor oscillations on TFTR. An oval-shaped hot spot is commonly seen in NBI heated plasmas

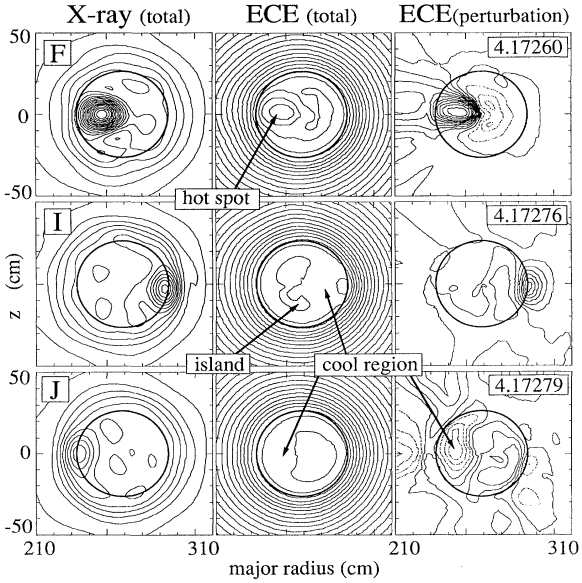

FIG. 3. Reconstructions of the x ray, the ECE, and the perturbation of ECE. The contour step size is 300 eV on ECE (total), and is 60 eV in frames F and I and 30 eV in frame J on ECE (perturbation), respectively. The plasma makes a half rotation from I to J.

and rf heated plasmas, but it has not been theoretically predicted [11].

The x-ray emission at the center decreases 75% during the sawtooth crash (the line integrated emission drops by 30%), which cannot be explained by the drop of the central electron temperature (10%) and density (10%). The detected x-ray spectrum is shown in Fig. 4(d). Before the sawtooth crash, the total $Z_{\rm eff}$ is 2.8 with a contribution from metals of $\sim$0.7. X-ray pulse-height analysis [12], which looks horizontally in the midplane, shows that the line averaged $\Delta Z_{\rm eff}$, the contribution from the metal impurities (iron, nickel, and chromium) to the $Z_{\rm eff}$, decreases 27%, as shown in Fig. 4(a). Time histories of the $\Delta Z_{\rm eff}$ and the x-ray emission correlate very well. The intensity of the $K\alpha$ resonance line of the heliumlike iron ion, Fe XXV, which is measured by a bent-crystal spectrometer [13], decreases 47%, as shown in Fig. 4(b). The observed drop of the electron temperature and density should reduce the Fe XXV line emission by 11%, as calculated by the MIST code [14]. Thus, the line averaged iron ion density must decrease $\sim$36%. The ratio of measured x-ray emission to calculated bremsstrahlung, based on measured temperature and density, is called the enhancement factor [15], and is an indicator of impurity content. In Fig. 4(c), it is observed that the enhancement factor profile becomes peaked between sawtooth crashes (t =4.1 s), and flattens after the sawtooth crash (t =4.2 s). These results show that the drastic x-ray drop at the sawtooth crash is due to the escape of the metal impurities, which have accumulated in the central region between crashes. The accumulation mechanism may be the high-Z ion pinch effect [16]. Just before the end of the sawtooth crash (Fig. 3, frame I), the x-ray emission in the hot spot is higher than in the island, although the electron temperature at the hot spot is equal to that at the island. These results indicate that the high x-ray emission in the hot spot is mainly due to the metal impurities.

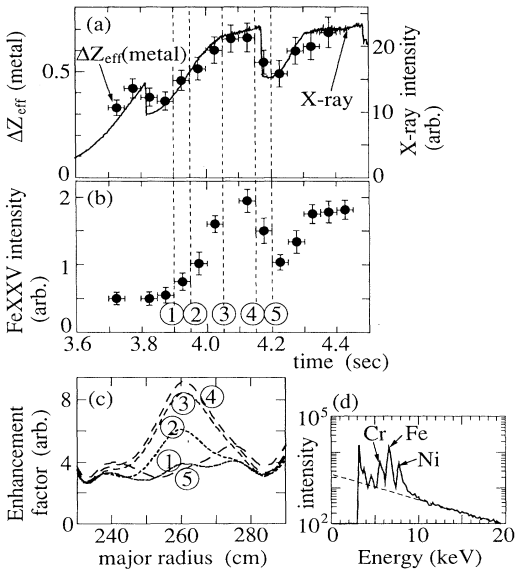

FIG. 4. (a) Time evolution of $Z_{\rm eff}$ due to the metal impurities (iron, nickel, and chromium), which is measured by the pulse-height analysis (PHA) x-ray spectrometer. The PHA data are averaged for 50 ms. The solid line is the x-ray emission from the central chord. (b) Time evolution of Fe XXV (0.185 nm) line emission which is measured by the crystal spectrometer. (c) Time evolution of the enhancement factor profile between the first sawtooth crash (t =3.9 s) and the second sawtooth crash (t =4.2 s). (d) X-ray spectrum measured by the PHA. The unit of the intensity is 3×10^{11} keV/keV cm^{2}s [12]. The three peaks are $K\alpha$ lines of metal impurities. The measured continuum (dotted line) is about 4 times higher than the calculated bremsstrahlung from a pure deuterium plasma.

Just after the crash (Fig. 3, frame J), a crescent-shaped "hot spot" remains in the x-ray image. This feature is also seen as a widely spread positive spike on the x-ray signal in the raw data traces (Fig. 1, 22 cm). This was also observed in the JIPP T-II tokamak, where it was interpreted as a kink flow along the q =1 surface [17]. On TFTR, however, the ECE electron temperature contours, which represent flux surfaces better than the x-ray emission contours, show a cool region. Therefore, this crescent-shaped x-ray contour does not show the kink flow; rather, it implies that the impurity transport time from the broken flux surface (X point) is much longer than the electron heat conduction time. Time scales can be estimated as follows: Particles and heat escape through the X point along the field line, at the electron thermal velocity v_e for the conduction and at the ambipolar velocity v_i for the convection; and each time scale is described by $\tau_a \approx (\pi R/v_a)q/\delta q$ (a =e,i), where δq is the change in q across the width of the reconnection layer and the suffices e and i indicate the electron heat conduction and the ion convection, respectively. For $\delta q/q$ =0.1, we have $\tau_e \approx 1$ μs and $\tau_i \approx 100$ μs, which explains the time lag of impurity contours related to the temperature contours.

The present experimental results lead to the following physical picture of the sawtooth crash. Since particles are frozen to the field line, the result that both impurities and heat escape through the X point from the inside to the outside of the inversion surface implies that field lines from inside and outside of the q =1 surface are reconnected during the sawtooth crash. The hot electrons escape to the outside and the cold electrons are drawn to the inside as a result of charge neutrality. Thus, the temperature of the reconnection region inside the original q =1 surface can be lower than the island, as is observed experimentally. The existence of the cool region implies that the island is not completely stochastic but that it has established flux surfaces.

In summary, simultaneous high-resolution ECE and x-ray image reconstructions have been made during the sawtooth crash in a fast rotating plasma with NBI heating on TFTR. The results suggest that the x-ray emission

describes the behavior of the metal impurities, the impurity convection is slow in comparison with the electron heat conduction, and the x-ray contours, such as the crescent hot spot at the end of the sawtooth crash, are therefore not representative of flux surfaces. The evolution of the electron temperature contours and the impurities behavior suggests that the sawtooth crash in the NBI heated TFTR plasma is a full reconnection process.

The authors would like to thank Dr. H. Park for the electron density measurements, and Dr. R. Büchse, Dr. P. Savrukhin, Dr. M. Zarnstorff, Dr. S. Scott, Dr. R. Budny, Dr. J. Schivell, Dr. A. Edwards, and Dr. J. Wesson for useful discussions. This work was supported by the U.S. DOE under Contract No. DE-AC02-76-CHO-3073.

---

[a]Permanent address: University of Tokyo, Tokyo 113, Japan.

[1] B. B. Kadomtsev, Fiz. Plazmy **1**, 710 (1975) [Sov. J. Plasma Phys. **1**, 389 (1975)].
[2] A. W. Edwards *et al.*, Phys. Rev. Lett. **57**, 210 (1986).
[3] J. A. Wesson, Nucl. Fusion **30**, 2545 (1990).
[4] A. Cavallo, R. C. Cutler, and M. P. McCarthy, Rev. Sci. Instrum. **59**, 889 (1988).
[5] F. J. Stauffer *et al.*, Rev. Sci. Instrum. **59**, 2139 (1988).
[6] Y. Nagayama *et al.*, Rev. Sci. Instrum. **61**, 3265 (1990).
[7] J. Kiraly *et al.*, Rev. Sci. Instrum. **56**, 827 (1985); K. W. Hill *et al.*, Rev. Sci. Instrum. **56**, 830 (1985).
[8] L. C. Johnson *et al.*, Rev. Sci. Instrum. **57**, 2133 (1986).
[9] Y. Nagayama, J. Appl. Phys. **62**, 2702 (1987).
[10] E. D. Fredrickson *et al.*, Phys. Rev. Lett. **65**, 2869 (1990).
[11] W. Park *et al.*, Phys. Fluids B **3**, 507 (1991).
[12] K. W. Hill *et al.*, Rev. Sci. Instrum. **56**, 840 (1985).
[13] K. W. Hill *et al.*, Rev. Sci. Instrum. **56**, 1165 (1985).
[14] R. A. Hulse, Nuclear Technology/Fusion **3**, 259 (1983).
[15] S. S. Sesnic *et al.*, J. Nucl. Materials **145-147**, 580 (1987).
[16] R. D. Petrasso *et al.*, Phys. Rev. Lett. **57**, 707 (1986).
[17] Y. Nagayama, S. Tsuji, and K. Kawahata, Phys. Rev. Lett. **61**, 1839 (1988).